Biophysical *Journal*
Biophysical Letter

Biophysical Society

Tectorial Membrane Traveling Waves Underlie Sharp Auditory Tuning in Humans

Shirin Farrahi,[1,2] Roozbeh Ghaffari,[1] Jonathan B. Sellon,[1,3] Hideko H. Nakajima,[4] and Dennis M. Freeman[1,2,3,*]
[1]Research Laboratory of Electronics and [2]Department of Electrical Engineering and Computer Science, Massachusetts Institute of Technology, Cambridge, Massachusetts; [3]Harvard-MIT Program in Health Sciences and Technology, Cambridge, Massachusetts; and [4]Department of Otolaryngology, Harvard Medical School and Massachusetts Eye and Ear, Boston, Massachusetts

ABSTRACT Our ability to understand speech requires neural tuning with high frequency resolution, but the peripheral mechanisms underlying sharp tuning in humans remain unclear. Sharp tuning in genetically modified mice has been attributed to decreases in spread of excitation of tectorial membrane traveling waves. Here we show that the spread of excitation of tectorial membrane waves is similar in humans and mice, although the mechanical excitation spans fewer frequencies in humans—suggesting a possible mechanism for sharper tuning.

The mammalian cochlea separates sounds by their frequency content, and this separation is critical to our ability to perceive speech, especially in acoustically challenging environments. While the cross-sectional structure of the mammalian organ of Corti is highly conserved across species, several studies have suggested that frequency selectivity has higher resolution (i.e., is more sharply tuned) in humans than in other mammals (1–3). Although sharper neural tuning in humans has been attributed to peripheral mechanisms (4–6), the origin of the difference in neural tuning remains unclear.

Recent in vitro and in vivo studies have revealed that the tectorial membrane (TM) contributes to spread of mechanical excitation via longitudinally propagating traveling waves (7–10). In particular, Tectb$^{-/-}$ mutant mice, which lack the β-tectorin glycoproteins, exhibit significantly sharper tuning (11). Furthermore, the spatial decay constant of TM waves in Tectb$^{-/-}$ mice is smaller by a factor of two (8), suggesting that differences in TM waves may underlie differences in neural frequency tuning observed in Tectb$^{-/-}$ mice. This result raises the possibility that neural frequency tuning in humans (4) may be sharper due in part to differences in TM longitudinal coupling and wave phenomena. Here we test this intriguing possibility by making, to our knowledge, the first direct measurements of fresh human TMs.

Temporal bones were harvested from human cadavers and mice, and midbasal TM segments were extracted and mounted in a wave chamber (Fig. 1 *a*) within 48 h postmortem. TM segments were stimulated mechanically to launch traveling waves (Movies S1 and S2 in the Supporting Material). Motion waveforms were captured using stroboscopic illumination with a custom computer vision technique (Materials and Methods). Measurements were performed in TM samples from mice for basal frequencies (>10 kHz) and from humans for basal frequencies (>5 kHz) subject to equipment limitations (<20 kHz), and representative displacement waveforms are superimposed on optical images of human and mouse TM segments in Fig. 1 *b*. TM wave decay constant, wavelength, and speed (Fig. 1 *c*) were computed from the magnitude and phase of TM radial displacements for both species (Fig. 1 *d*).

Our measured wave decay constants (σ) and speeds (v) are similar in humans and mice. The speed of TM traveling waves in human samples increases by roughly a factor of two from 5 to 20 kHz. Mouse TM speeds also increase with frequency, nearly overlapping human speeds for the physiologically relevant range of frequencies (10–20 kHz). The median decay constants of human TMs range from 150 and 450 μm from 5 to 20 kHz and are relatively constant with frequency. Similarly, the range of median σ-values for mouse TMs is 80–300 μm from 10 to 20 kHz. We see significant overlap of the median and ranges between the two species over their common frequency range of basal hearing (10–20 kHz; Fig. 1 *d*).

Wave properties of viscoelastic solids depend on the solid's material properties, including density ρ, shear storage modulus G', and shear viscosity η (7). To account for boundary conditions in the wave chamber, we used a lumped parameter model consisting of a distributed series

Submitted May 24, 2016, and accepted for publication July 20, 2016.
*Correspondence: freeman@mit.edu
Editor: James Keener.
http://dx.doi.org/10.1016/j.bpj.2016.07.038

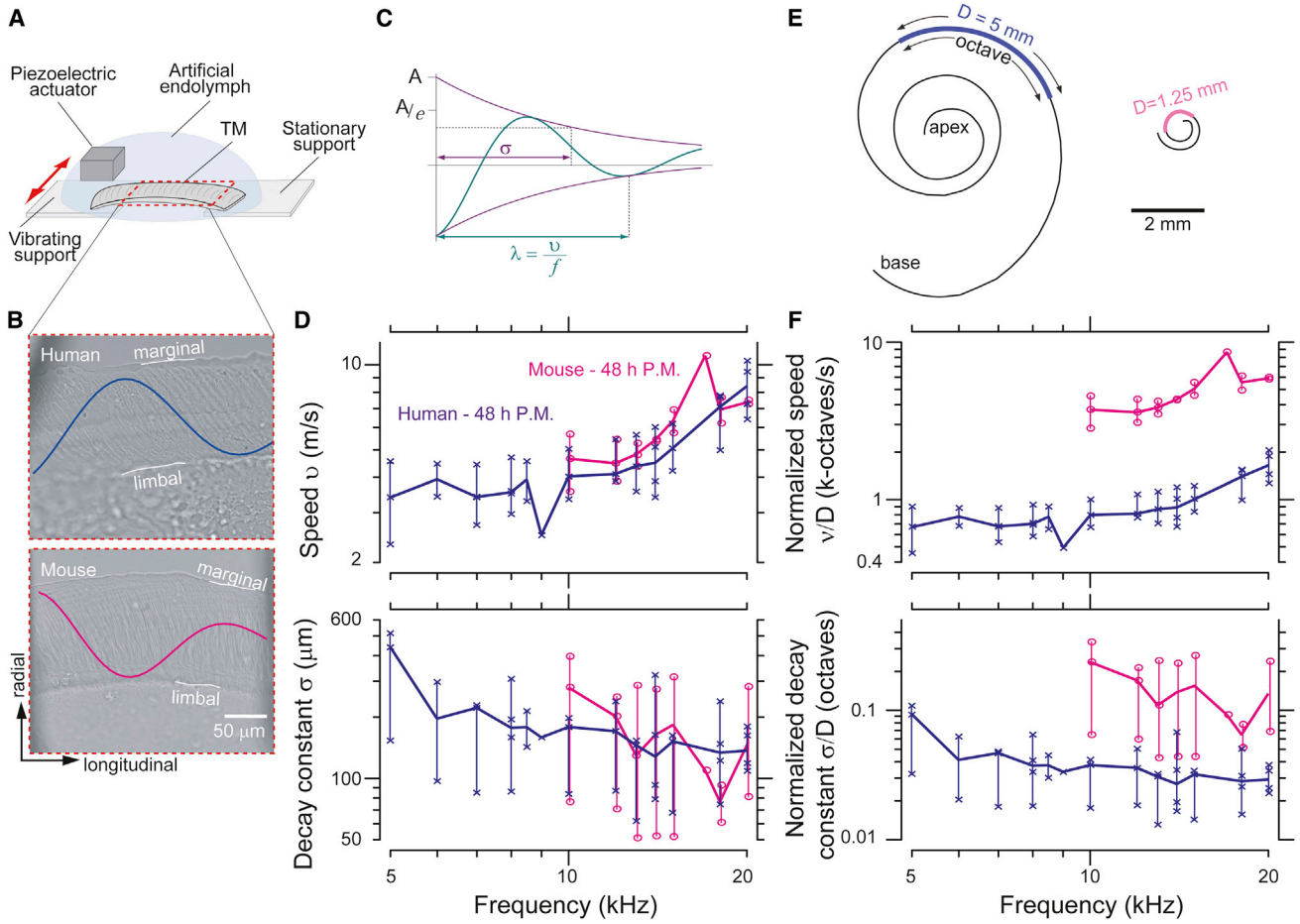

FIGURE 1 (***A***) **Wave chamber used to deliver sinusoidal mechanical stimulation in the radial direction to launch traveling waves along excised TM segments. (*B*) Light microscope images of human and mouse TMs in a wave chamber. Waveforms superimposed on the image show radial motion exaggerated to help visualize the motion in response to 8 kHz (human) and 15 kHz (mouse) stimuli. Marginal and limbal boundaries of the TM are indicated. (*C*) TM wave properties analyzed from the motion waveforms include wavelength (λ), speed (v), and wave decay constant (σ). (*D*) Frequency dependence of traveling wave speeds (*top*) and TM wave decay constants (*bottom*) for human and mouse basal segments. (*E*) Schematic drawings of cochlear spirals in human and mouse. The spatial extents of octave intervals (as calculated from the cochlear maps of Greenwood (12) and Müller et al. (13)) are indicated with colored lines along the spiral. (*F*) TM wave speeds and decay constants divided by *D*, the distance over which frequency changes by an octave for each species. Symbols indicate all data points. (*Thick horizontal lines*) Medians; (*vertical lines*) range of data measured at a single frequency across preparations (human, $n = 4$; mouse, $n = 4$).**

of masses coupled by viscous and elastic elements (7). We computed the material properties for each TM wave measurement and found no significant difference between human ($G' = 14.5 \pm 8.2$ kPa and $\eta = 0.16 \pm 0.1$ Pa·s) and mouse ($G' = 16.3 \pm 6.6$ kPa and $\eta = 0.21 \pm 0.1$ Pa·s) material properties.

The spatial decay constants for both mice and humans are on the order of 150 μm at 20 kHz (Fig. 1 *e*). This distance is a measure of longitudinal spread of excitation and correlates with spectral spread of excitation (7). Each cochlear location is mechanically excited not only by its best frequency, but also by frequencies that best excite adjacent regions with different best frequencies. For mice, the spatial spread of 150 μm corresponds to a frequency spread of 1.6 kHz and therefore a quality of tuning Q_{10dB} of approximately 10 at 20 kHz (8). In TectB knockout mice, the decay constant of TM waves is approximately halved, leading to a Q_{10dB} value that is doubled (8). This sharpened tuning, predicted from the mechanical spread of excitation measured in an isolated TM, correlates well with sharpened tuning in auditory nerve measurements of these mutant mice (11).

While TM waves spread excitations over similar distances in mice and humans, these distances span significantly different ranges of frequencies (Fig. 1 *e*). For the mouse, the 150-μm decay constant represents a frequency range of >1.4 kHz, while the same distance corresponds to <300 Hz in humans (Fig. 1 *f*). This difference has important implications for our ability to separate sounds by their frequency content—suggesting that the spread of excitation via TM traveling waves is broader in mice than in humans. It

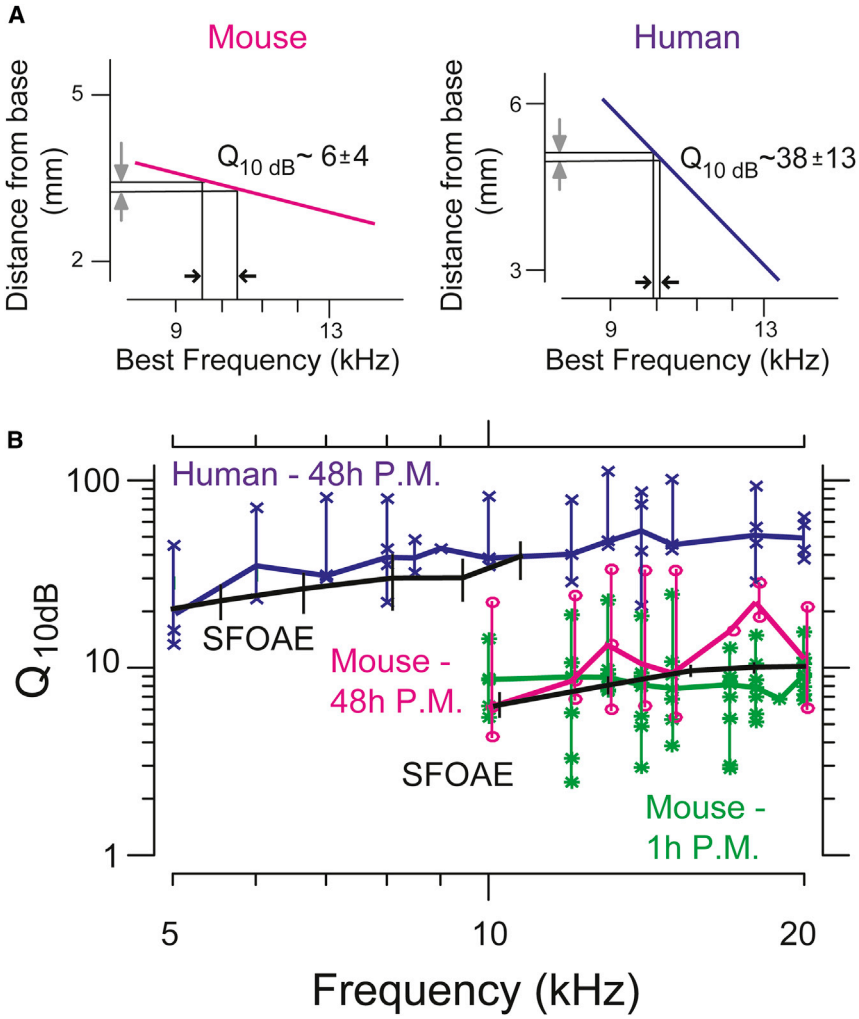

FIGURE 2 (***A***) Place-frequency maps for mouse (***left***) and human (***right***) showing how TM wave decay constants relate to frequency bandwidth of tuning. (***B***) Estimates of Q_{10dB} for human (***blue***, $n = 4$) and mouse (***magenta***, $n = 4$) from TM waves compared to published stimulus frequency otoacoustic emission data (***SFOAE***, ***black lines***; mouse (14), human (15)). Also plotted in green are estimates of Q_{10dB} from mouse TM wave measurements performed within 1 h postmortem. Symbols indicate all data points. (***Thick horizontal lines***) Medians; (***vertical lines***) range of data measured at a single frequency for all samples (human, $n = 4$; mouse 48 h postmortem, $n = 4$; mouse 1 h postmortem, $n = 10$).

is therefore important to characterize spread of excitation in terms of the range of frequencies over which the excitation is spread. Because the relation between cochlear location and best frequency is approximately logarithmic (Fig. 2 *a*) (12,13), constant distances map to logarithmic frequency ranges, such as octaves. We therefore converted TM wave decay constants from distances (in meters) to frequency ranges (in octaves) by dividing σ by the distance D over which frequency changes by one octave. The resulting normalized decay constants for mice and humans differ significantly (Fig. 2 *a*), with those for humans being ~4 times smaller than those for mice. Thus, normalizing the wave decay constant to reflect the physiologically important range of frequencies reveals striking differences between humans and mice.

The ratio of the center frequency to the range of frequencies coupled by the TM wave decay constant defines a quality of tuning (Q_{10dB}). Fig. 2 *b* shows significantly larger quality of tuning in humans compared to mice (larger by a factor of five), consistent with a smaller spatial extent of TM waves relative to the cochlear map. These Q_{10dB} predictions based on TM wave decay constants are comparable to cochlear tuning predictions based on otoacoustic emissions (4). Previous studies have shown these emission-based estimates of tuning to be comparable to neural estimates for a range of mammalian species (4–6). For mice, the quality of tuning estimated from TM wave decay constants closely matches predictions of Q_{10dB} from otoacoustic emissions (14). For humans, the Q_{10dB} estimates are comparable to emissions-based estimates (15) from 5 to 10 kHz. Taken together, these findings suggest that the spatial extent of TM waves strongly correlates with cochlear tuning in humans, mice, and likely other mammals. This correlation suggests that spread of excitation through TM traveling waves contributes to differences in tuning in humans and other mammals.

SUPPORTING MATERIAL

Supporting Materials and Methods, two figures, and two movies are available at http://www.biophysj.org/biophysj/supplemental/S0006-3495(16)30618-X.

AUTHOR CONTRIBUTIONS

S.F., R.G., and D.M.F. designed the research; S.F. and H.H.N. conducted the work on human temporal bones; S.F. and J.B.S. conducted the experiments on mice and analyzed the data; and S.F., R.G., and D.M.F. wrote the article.

ACKNOWLEDGMENTS

The authors thank Diane Jones for dissecting the human temporal bones from donors. We also thank Christopher A. Shera, John J. Guinan Jr., and Scott L. Page for their helpful comments and suggestions on this work.

This research was supported by National Institutes of Health grant No. R01-DC00238. S.F. and J.B.S. were supported in part by a training grant from the National Institutes of Health to the Speech and Hearing Biosciences and Technology Program in the Harvard-MIT Program in Health Sciences and Technology.

REFERENCES

1. Bitterman, Y., R. Mukamel, …, I. Nelken. 2008. Ultra-fine frequency tuning revealed in single neurons of human auditory cortex. *Nature.* 451:197–201.
2. Harrison, R. V., J.-M. Aran, and J.-P. Erre. 1981. AP tuning curves from normal and pathological human and guinea pig cochleas. *J. Acoust. Soc. Am.* 69:1374–1385.
3. Sinnott, J. M., M. D. Beecher, …, W. C. Stebbins. 1976. Speech sound discrimination by monkeys and humans. *J. Acoust. Soc. Am.* 60:687–695.
4. Shera, C. A., J. J. Guinan, Jr., and A. J. Oxenham. 2002. Revised estimates of human cochlear tuning from otoacoustic and behavioral measurements. *Proc. Natl. Acad. Sci. USA.* 99:3318–3323.
5. Shera, C., J. Guinan, Jr., and A. Oxenham. 2010. Otoacoustic estimation of cochlear tuning: validation in the chinchilla. *J. Assoc. Res. Otol.* 11:343–365.
6. Joris, P. X., C. Bergevin, …, C. A. Shera. 2011. Frequency selectivity in Old-World monkeys corroborates sharp cochlear tuning in humans. *Proc. Natl. Acad. Sci. USA.* 108:17516–17520.
7. Ghaffari, R., A. J. Aranyosi, and D. M. Freeman. 2007. Longitudinally propagating traveling waves of the mammalian tectorial membrane. *Proc. Natl. Acad. Sci. USA.* 104:16510–16515.
8. Ghaffari, R., A. J. Aranyosi, …, D. M. Freeman. 2010. Tectorial membrane travelling waves underlie abnormal hearing in Tectb mutant mice. *Nat. Commun.* 1:96.
9. Sellon, J. B., S. Farrahi, …, D. M. Freeman. 2015. Longitudinal spread of mechanical excitation through tectorial membrane traveling waves. *Proc. Natl. Acad. Sci. USA.* 112:12968–12973.
10. Lee, H. Y., P. D. Raphael, …, J. S. Oghalai. 2015. Noninvasive in vivo imaging reveals differences between tectorial membrane and basilar membrane traveling waves in the mouse cochlea. *Proc. Natl. Acad. Sci. USA.* 112:3128–3133.
11. Russell, I. J., P. K. Legan, …, G. P. Richardson. 2007. Sharpened cochlear tuning in a mouse with a genetically modified tectorial membrane. *Nat. Neurosci.* 10:215–223.
12. Greenwood, D. D. 1990. A cochlear frequency-position function for several species—29 years later. *J. Acoust. Soc. Am.* 87:2592–2605.
13. Müller, M., K. von Hünerbein, …, J. W. Smolders. 2005. A physiological place-frequency map of the cochlea in the CBA/J mouse. *Hear. Res.* 202:63–73.
14. Cheatham, M. A., R. J. Goodyear, …, J. H. Siegel. 2015. Mechanics of Hearing: Protein to Perception. *In* Proceedings of the 12th International Workshop on the Mechanics of Hearing. K. D. Karavitaki and D. P. Corey, editors. American Institute of Physics, Melville, NY.
15. Dreisbach, L. E., J. H. Siegel, and W. Chen. 1998. Vector decomposition of distortion product otoacoustic emission sources in humans. *J. Assoc. Res. Otolaryngol. Abstr.* 21:347.

Biophysical Journal, Volume *111*

Supplemental Information

Tectorial Membrane Traveling Waves Underlie Sharp Auditory Tuning in Humans

Shirin Farrahi, Roozbeh Ghaffari, Jonathan B. Sellon, Hideko H. Nakajima, and Dennis M. Freeman

Supplementary material for 'tectorial membrane traveling waves underlie sharp auditory tuning in humans'

Shirin Farrahi,*,† Roozbeh Ghaffari, * Jonathan B. Sellon, *,‡ Hideko H. Nakajima,¶ and Dennis M. Freeman*,†,‡

*Research Laboratory of Electronics, Massachusetts Institute of Technology, Cambridge, Massachusetts 02139, USA; †Department of Electrical Engineering and Computer Science, Massachusetts Institute of Technology, Cambridge, MA 02139, USA; ‡Harvard--MIT Program in Health Sciences and Technology, Cambridge, MA 02139, USA; ¶Department of Otolaryngology, Harvard Medical School and Massachusetts Eye and Ear, Boston, MA, 02114, USA

MATERIALS AND METHODS

Extraction of human TM samples

Human temporal bones were obtained from the Massachusetts Eye and Ear Temporal Bone Bank. Temporal bones were removed within 24 hours post mortem and were refrigerated in 0.9% normal saline for several hours before being transferred to a bath of artificial endolymph (AE) containing 174 mM KCl, 5 mM Hepes, 3 mM dextrose, 2 mM NaCl, and 0.02 mM $CaCl_2$. The bath was titrated to pH 7.2 using small quantities of KOH or HCl as necessary. Preparation of the specimen was performed using universal precautions. After opening the facial recess, the round window and stapes were exposed, and the incudo-stapedial joint was severed to allow removal of the tympanic membrane and middle ear cavity without disrupting the inner ear. Surgical drilling took approximately three hours to expose the cochlea and thin the bone near the region covering the organ of Corti while the specimen was kept moist with AE. Once the outline of the cochlear spiral was sufficiently thinned and the specimen well rinsed of bone dust, the remaining bone around the cochlear spiral was removed using a scalpel blade (no. 11) and curved surgical scissors under a dissection microscope (Wild Hexagon, Stockholm, Sweden). Once the bone around the cochlea was opened, the cochlea was kept in AE. Stria vascularis was removed using fine forceps, and a needle (26 ga) was used to extract the organ of Corti from along the cochlear spiral starting from the base. The TM was gently removed from the surface of the organ of Corti using a sterilized eyelash. TM segments were photographed to identify their origin along the cochlea then were cut into 1-2 mm segments using a needle. TM segments from the basal turn were transferred to a clean AE bath using a glass-tipped pipette, then were used for wave measurements as described below. In one human bone that was used for training, the entire cochlear spiral was exposed (Suppl. Fig 1) showing the basal, middle, and apical turns of the human cochlea. A total of 15 temporal bones were used in the development of the measurement techniques, and results were obtained from an additional 3 temporal bones.

Human TM wave properties could not be measured immediately after death. All measurements shown here were performed roughly 48 hours post mortem. We performed a study in mice to measure the changes in mouse TM wave properties when treated in a similar fashion to humans. We found that mouse TM wave decay constants were almost indistinguishable in samples dissected 48 hours post mortem compared to samples measured 1 hour post mortem (Suppl. Fig. 2).

Extraction of mouse TM samples

Mice were euthanized by carbon dioxide asphyxiation, followed by decapitation. All mouse TMs were extracted in a similar manner to that used in human TM extraction. To this end, heads were refrigerated overnight after which temporal bones were extracted and bullae were opened and placed in 0.9% saline. After several hours, cochleae were dissected and placed in an artificial endolymph bath as described above for humans. An example mouse cochlea is included in Supplementary Figure 1. The cochleae were refrigerated in AE until approximately 36 hours after the animal's time of death, at which point the cochleae were dissected using a scalpel blade (no. 11) and TM samples were extracted using a sterilized eyelash. TM wave measurements were performed approximately 48 hours post mortem to mimic the human condition as closely as possible.

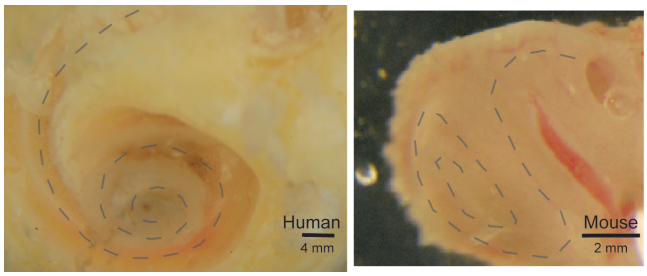

Figure 1: Light microscope images of human (left) and mouse (right) cochleae.

Measurement of TM wave properties

TM waves were measured optically as described by Ghaffari et al (1). Briefly, isolated TM segments were suspended between two supports using Cell Tak bioadhesive (Collaborative Research, Bedford, MA). One of the supports was glued down and thus remained stationary while the other was attached to a piezo-electric

actuator (Thorlabs Inc., Newton, NJ). The TM was stimulated in the radial cochlear direction, and motions along its surface were measured at frequencies in the basal range for mice (>10 kHz) and humans (>5 kHz), subject to the maximum frequency of our amplifier (<20 kHz). Samples were optically inspected to eliminate those that were damaged during the isolation process or improperly mounted. Experiments were performed at MIT and approved by MIT's Committees on Animal Care and Environmental Health and Safety.

Motion amplitude and phase were measured using a stroboscopic computer vision technique that allows images to be captured at several phases of motion (2). Radial TM displacement and phase were determined from a one-dimensional fast Fourier transform (FFT) taken at evenly spaced points along the TM. Spatial decay constant, σ, was defined as the distance in μm along the TM over which the wave magnitude decays by a factor of *e*. The σ values for each TM were determined by fitting an exponential to the overall magnitude of the response along the TM. Speed, *v*, was determined by fitting a straight line to the phase as a function of distance along the TM and multiplying the verse slope by angular frequency.

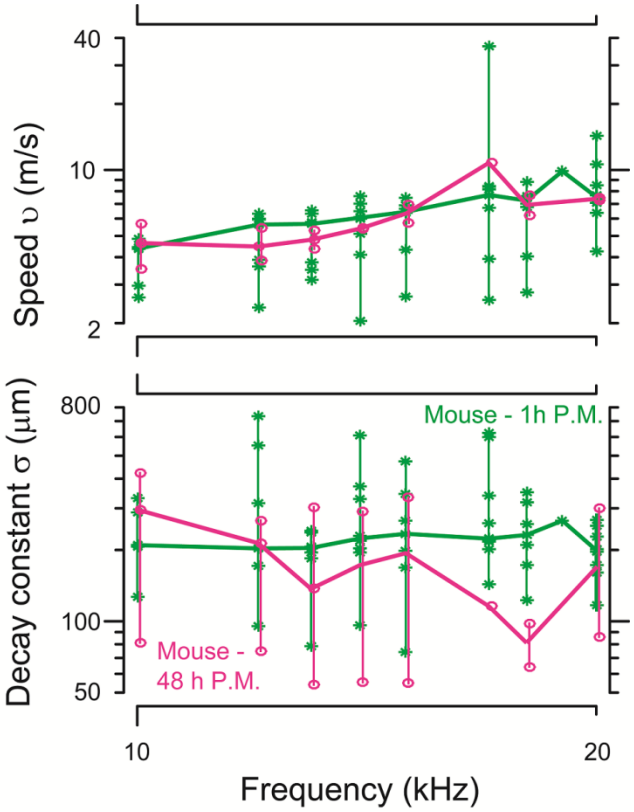

Figure 2: Wave speeds (top) and decay constants (bottom) in freshly dissected (1 hour post-mortem, n = 10) and aged (48 hours post-mortem, n = 4) mouse TMs from 10 to 20 kHz. Symbols indicate all data points. Thick horizontal lines indicate medians, and vertical lines indicate range of all data points at a single frequency.

SUPPLEMENTARY FIGURE AND VIDEOS

Human TM measurements were performed approximately 48 hours post-mortem in this study. To study the impact of this aging on TM wave properties, we aged several mouse temporal bones in a similar manner to the human temporal bones and compared these measurements to freshly dissected mouse TM waves. As shown in Supplementary Figure 2, we did not see significant differences in wave properties due to this aging of mouse temporal bones ($p = 0.01$). We therefore concluded that the human TM measurements shown in this study were a close representation of the wave properties we would see if it were possible to dissect and measure human TMs sooner after death.

Also included here are two videos of human and aged mouse TM waves from samples that were included in this study. In these videos, we magnified the TM motions by a factor of 20 using a phase based method (2) to see the motions more easily. The videos show motions at 20 kHz. These videos were used for comparison with measurements of TM wave properties presented in Figure 1, which were analyzed using computer microvision algorithms (3).

References

1. Ghaffari, R., A. J. Aranyosi, and D. M. Freeman, 2007. Longitudinally propagating traveling waves of the mammalian tectorial membrane. Proc. Nat. Acad. Sci. USA 104:16510–16515.
2. Wadhwa, N., M. Rubinstein, F. Durand, and W. Freeman, 2013. Phase-based video motion processing. ACM TOG 32:80
3. Davis, C. Q., and D. M. Freeman, 1998. Using a light microscope to measure motions with nanometer accuracy. Opt. Eng. 37:1299–1304.